

Geophysical Research Letters®



RESEARCH LETTER

10.1029/2025GL116902

Key Points:

- We simulate the evolution of water properties in 37 Greenlandic fjords using a computationally efficient reduced physics model (FjordRPM)
- Subglacial discharge plumes reduce temperature stratification relative to the shelf, while iceberg melting cools surface waters
- The model reproduces observed fjord properties in NW Greenland, while larger errors in the SE are likely linked to shelf boundary conditions

Supporting Information:

Supporting Information may be found in the online version of this article.

Correspondence to:

M. Mas e Braga,
mabrag@bas.ac.uk

Citation:

Mas e Braga, M., Cowton, T., Slater, D., Inall, M., Johnstone, E., & Fraser, N. (2025). Controls on fjord temperature throughout Greenland in a reduced-physics model. *Geophysical Research Letters*, 52, e2025GL116902. <https://doi.org/10.1029/2025GL116902>

Received 16 MAY 2025

Accepted 20 AUG 2025

Author Contributions:

Conceptualization: Martim Mas e Braga, Tom Cowton

Data curation: Martim Mas e Braga

Formal analysis: Martim Mas e Braga

Funding acquisition: Tom Cowton

Investigation: Martim Mas e Braga

Methodology: Martim Mas e Braga, Tom Cowton

Project administration: Tom Cowton, Donald Slater, Mark Inall

Resources: Tom Cowton

Software: Martim Mas e Braga, Donald Slater, Eleanor Johnstone

Validation: Martim Mas e Braga






Visualization: Martim Mas e Braga

Writing – original draft: Martim Mas e Braga

© 2025. The Author(s).

This is an open access article under the terms of the [Creative Commons Attribution License](#), which permits use, distribution and reproduction in any medium, provided the original work is properly cited.

Controls on Fjord Temperature Throughout Greenland in a Reduced-Physics Model

Martim Mas e Braga^{1,2} , Tom Cowton¹ , Donald Slater³ , Mark Inall⁴ , Eleanor Johnstone³, and Neil Fraser⁴ 

¹School of Geography and Sustainable Development, University of St Andrews, St Andrews, UK, ²Now at British Antarctic Survey, Cambridge, UK, ³School of Geosciences, University of Edinburgh, Edinburgh, UK, ⁴Scottish Association for Marine Science, Scottish Marine Institute, Argyll, UK

Abstract Greenland's fjords modulate exchanges between its outlet glaciers and the open ocean. Subglacial discharge and iceberg melt redistribute heat and salt in the fjord, modifying waters at glacier fronts and impacting glacier melt. Considering observations are sparse and general circulation models are computationally expensive, we use a reduced-physics model to simulate vertical profiles of temperature and salinity for 37 fjords around Greenland. For each fjord, we conduct large model ensembles to explore the effects of subglacial discharge, iceberg melt, and fjord-shelf exchange on water properties. We show that our model successfully captures water mass changes inside fjords: iceberg melt cools the surface, while subglacial discharge plumes and fjord-shelf exchange tend to decrease and increase temperature stratification, respectively. By comparing our ensemble to observations, we highlight that despite high interannual and fjord-to-fjord variability in ocean and meltwater forcings, a reduced-physics model can elucidate how fjords modulate ice-sheet-ocean exchanges at Greenland-wide scales.

Plain Language Summary Greenland's fjords control how the ice sheet and the open ocean exchange water properties with each other. Meltwater discharge from the ice sheet and melting icebergs mix with ambient fjord waters, changing their temperature and salinity, therefore affecting how much they can melt glaciers. Here we use a simple model to simulate several Greenland fjords and show that high iceberg melting cools the fjord, whereas ice-sheet meltwater discharge homogenizes the fjord (either warming or cooling it depending on which water masses are mixed), while increased fjord communication with the continental shelf reduces the effect of these processes. We further use available measurements to compare with our results and find common values of model parameters that can be used to simulate fjords that have no available data.

1. Introduction

The Greenland Ice Sheet (GrIS) holds enough freshwater to raise global mean sea level by ~7.5 m if melted completely (Morlighem et al., 2017), with the potential to alter ocean circulation (Böning et al., 2016). About 70% of GrIS mass loss over recent decades has occurred through marine-terminating (also known as tidewater) outlet glaciers (Mouginot et al., 2019). Tidewater glaciers often drain into fjords, which are deep, narrow, and long bodies of water that connect the ice sheet to the continental shelf. Water properties in these fjords are thus an important control on GrIS mass loss.

Fjord water properties are determined by the properties of ocean waters entering the fjord from the continental shelf (hereafter, “the shelf”) and processes acting to modify these waters within the fjords themselves. In general, shelf waters are characterized by a shallow seasonally variable surface layer overlying a relatively cool and fresh Polar Water (PW) layer, which in turn sits above a layer of warmer and saltier Atlantic Water (AW; Straneo et al., 2012). The properties of waters entering fjords may vary over time in response to variability in shelf water properties, but also between fjords depending on the ease of exchange between the fjord and shelf, which in turn can be influenced by bathymetric constraints such as the presence of shallow sills (Figure 1a; Jakobsson et al., 2020; Millan et al., 2018).

Within fjords, water properties are influenced by the input of freshwater from the GrIS in the form of both liquid meltwater and icebergs. Most meltwater drains to the ice sheet bed, and is discharged deep below sea level at tidewater glaciers (Chu, 2014). Being fresh and thus less dense than ambient fjord waters, it rises as a buoyant plume, entraining ambient waters (I in Figure 1a) until it either reaches neutral buoyancy or the surface, resulting

Writing – review & editing:
Tom Cowton, Donald Slater, Mark Inall,
Neil Fraser

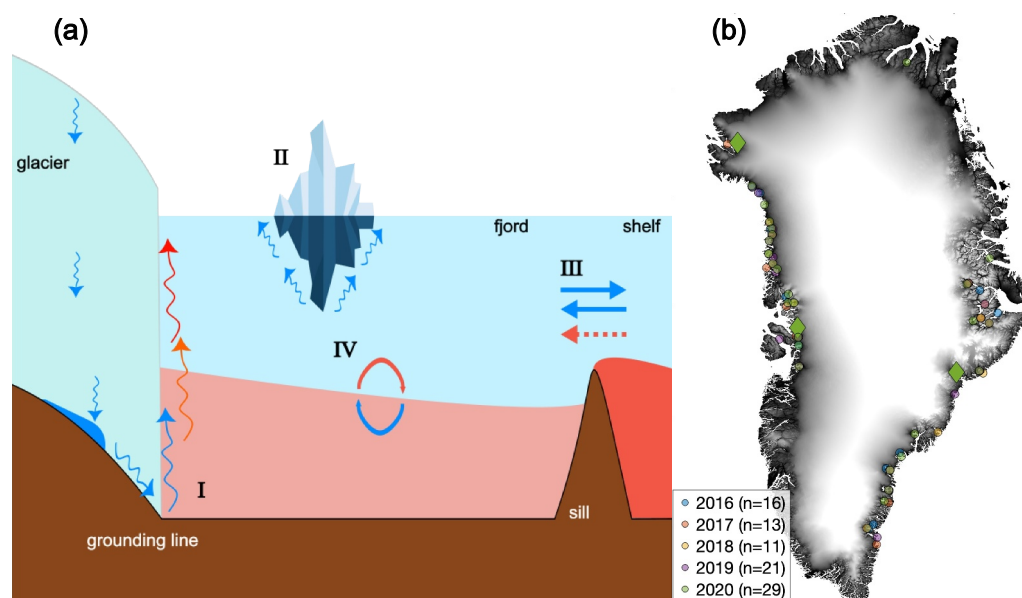


Figure 1. (a) Summary of processes affecting fjord temperatures investigated in this work: (I) subglacial meltwater plume, (II) iceberg melt, (III) fjord-continental shelf exchanges; (IV) internal mixing (not investigated in this work, but included in the model). (b) Simulated Greenland fjords for each year (colors). Larger diamond markers highlight the fjords discussed in the text and shown in Figures 2 and 3. The number of simulated fjords in each year (n) is shown in the legend.

in mixing and upwelling of deep waters (De Andrés et al., 2020; Jackson et al., 2017; Mankoff et al., 2016; Mortensen et al., 2020). Meanwhile, calving creates icebergs, which cool the fjord surface (II in Figure 1a), whilst also driving smaller meltwater plumes around them (Cenedese & Straneo, 2023; Davison et al., 2022). As a result of these processes, the water mass structure near the ice front is often different from the shelf (Cowton et al., 2023; Inall et al., 2014).

Studying oceanographic processes in a fjord is however challenging. Few fjords have been extensively surveyed due to inaccessibility, and data coverage, where available, is short in time and restricted to recent decades (Straneo & Cenedese, 2015). Our lack of understanding of Greenlandic fjords behavior is further exacerbated because global climate models are too coarse to resolve fjords, and regional ocean models that simulate such fjords are computationally expensive, restricting simulations to specific fjords and short, seasonal-to-interannual simulations (e.g., Cowton et al., 2016; Fraser & Inall, 2018; Sanchez et al., 2024), with few longer-timescale examples (Wood et al., 2024). For this reason, ice-sheet models often use oceanographic data from the shelf to parameterize submarine melt at tidewater glaciers (Nowicki et al., 2020; Slater et al., 2019, 2020). Consequently, fjord dynamics that modulate heat delivery to glacier fronts (Jackson et al., 2022; Mortensen et al., 2020; Sutherland & Straneo, 2012) are mostly overlooked, with implications for the accuracy of glacier melt-rate estimates (Hager et al., 2024).

To address this problem, we have recently developed a fjord model that incorporates key processes while remaining sufficiently efficient to be applicable at an ice sheet-wide scale (Slater et al., 2025). This Fjord Reduced-Physics Model (FjordRPM) has been shown to successfully capture intermediary and buoyancy-driven circulation under constant and transient forcings in idealized scenarios (Slater et al., 2025). Here we build upon these idealized simulations and apply the model to 37 of Greenland's ~150 glacial fjords, with a particular focus on their vertical temperature structure, given its likely importance in determining submarine melt. The aims of this research are (a) to assess the ability of FjordRPM to capture the observed modification of fjord water properties due to in-fjord processes across a wide range of real-world fjords; (b) to explore the relative impact of the different fjord processes on the fjord vertical temperature structure; and (c) to assess the sensitivity of these impacts to uncertain ice-ocean and circulation-related model parameters.

2. Methods

2.1. Model

FjordRPM is a “1.5-dimensional” model (i.e., a 1-dimensional model with lateral fluxes) that represents a fjord as a set of N vertically-stacked layers (here, $N = 60$) whose temperature and salinity evolve in time according to parameterized exchange processes. These include (I) exchange with subglacial discharge plume(s) driven by entrainment and intrusion, (II) exchange with icebergs through melting and melt-driven upwelling, (III) exchange with the shelf driven by density gradients, and (IV) exchange between layers due to vertical mixing and advection (Figure 1a). For a full description of the model, see Slater et al. (2025).

2.2. Data

To run the model, we require knowledge of (a) fjord geometry, (b) subglacial discharge and (c) contemporaneous shelf (for forcing) and fjord (for validation) temperature and salinity profiles. We digitize 151 fjords around Greenland based on available bathymetry (BedMachine) and coastline data (Gerrish, 2020; Morlighem, 2022), excluding fjords where no glaciers are grounded below 50 m depth. We refer to fjords by their digitised ID and/or their native name (ASIAQ Greenland Survey, accessed on 2023-08-24), as provided in QGreenland (Figure S1 in Supporting Information S1; Moon et al., 2023) and included in Mas e Braga (2025a). For each fjord, we compile estimated subglacial discharge timeseries (Karlsson et al., 2023). Where multiple glaciers discharge into a single fjord, we amalgamate all subglacial discharge into a single input discharged at the deepest grounding line in that fjord. To obtain fjord and shelf conditions, we utilize CTD casts from Oceans Melting Greenland (Fenty et al., 2016; OMG, 2019, 2020), identifying 90 instances, across 37 fjords, in which contemporaneous fjord and shelf casts are available (Figure 1b). Shelf profiles were either taken directly at the fjord mouth or in a trough slightly upstream from it (with respect to typical shelf currents). A single fjord-shelf cast pair was chosen for each year, and all were taken during summers (mostly during August/September). We refer to a fjord with a pair of in-fjord and shelf CTDs for a certain year as a “fjord-year combination”. Each of these 90 fjord-year combinations then forms the basis for an ensemble of model runs. We treat each year as a standalone experiment and simulate only years in which data is available—for example, a fjord may be simulated for 2016 and 2018, but not 2017.

2.3. Experiment Design

For each fjord, we use the corresponding year's shelf CTD data as initial conditions for both shelf and fjord, then simulate the evolution of fjord properties in response to the imposed subglacial discharge and iceberg melt. Shelf boundary conditions are likewise based on the shelf CTD data and are kept constant throughout; while this misses seasonal variation in shelf water properties, we deem this preferable to the significant error that would be introduced by forcing the model using ocean reanalyses, which struggle to capture the water mass structure on the Greenland shelf (Uotila et al., 2019). We perform a 10-year spin up (comprising 10 repeated annual runoff cycles) in each simulation, necessary to allow slowly changing layers (i.e., those below sill depth) to reach quasi-equilibrium conditions following initiation with shelf water properties. Most changes, however, happen over the first 2–3 years (Figures S2–S6 in Supporting Information S1).

For each fjord, we run an ensemble of simulations varying three key FjordRPM parameters. We do this because these parameters remain poorly constrained by observations, and because evaluating the response of the model to varying these parameters provides insight into the impacts of associated processes. The first is the submerged iceberg area (A_0); for a given iceberg melt rate, greater submerged area gives higher meltwater fluxes and increased cooling and freshening of the fjord. Given that there is also uncertainty in the scaling between fjord temperature and iceberg melt rate (Slater et al., 2025), A_0 can more broadly be seen as controlling the iceberg meltwater flux for given fjord properties. Nevertheless, it is important to highlight that iceberg melt is vertically resolved, with A_0 being the vertically integrated area following Equation 1 in Text S1 of Supporting Information S1. The second is the subglacial discharge plume width (W_p); for a given subglacial discharge, wider plumes give higher upwelling fluxes but reach neutral buoyancy at greater depths. The third is the fjord-shelf exchange coefficient (C_0); for a given fjord to shelf density gradient, which varies with depth, C_0 linearly scales the exchange flux between the fjord and shelf in each model layer. A_0 and W_p are potentially observable, while C_0 is more of a tuning parameter.

To assess the uncertainty around these three parameters, we produce different sets ($n = 300$) by Latin Hypercube Sampling (LHS), which randomly samples each variable from uniform distributions, and is able to efficiently cover the parameter space with a smaller sample size than a Monte Carlo approach (Song & Kawai, 2023). Each set is applied to the 90 fjord-year combinations, giving 27,000 simulations in total. The minimum and maximum values for W_p and C_0 (10–700 m and $50\text{--}5 \cdot 10^5 \text{ s}^{-1}$, respectively) are chosen as the widest range that yields stable model runs using a 1-hr time step. A_0 was varied from zero to a value 50% higher than mean estimates of iceberg-heavy fjords like Sermilik and Ilulissat ($4.5 \times 10^8 \text{ m}^2$; Enderlin et al., 2016), with these exaggerated upper values allowing for uncertainty in iceberg melt rates, which may in reality be higher than in the model. We perform another set of simulations using a smaller fjord ensemble covering a wider range of parameter values where all parameters are varied independently, which shows our chosen range was sufficient to capture the optimal range of parameter values (Figure S7 in Supporting Information S1). To highlight the effects of the main processes, we additionally run a set of experiments with each process absent (i.e., no icebergs, no subglacial discharge, or a decrease in fjord-shelf exchange by almost three orders of magnitude) and mid-range values for the remaining parameters.

Finally, within each ensemble, all 300 runs are compared with their respective fjord CTD profiles at the same time of the year. Since most observations were taken in early September, we opt for a 10-day average in early September (Text S1 in Supporting Information S1) as our modeled profile for comparison. For each ensemble, we find the ensemble member with the parameter combination that best matches observations. We do so by computing, for each ensemble member, the root mean square error (RMSE) between observed and modeled fjord profiles for both temperature and salinity. These RMSE values are then normalized by dividing by the observed range of temperature or salinity values respectively across all in-fjord profiles, and then averaged to give a combined RMSE value for each ensemble member. Our best ensemble member is then the one with the smallest combined RMSE. By this method we select an ensemble member that provides a good fit to both temperature and salinity, equally weighted.

3. Results and Discussion

3.1. Fit to Observations

In most cases, FjordRPM successfully reproduces the observed temperature and salinity profiles, closely matching observed fjord properties within the simulated parameter range (Figure 2; Supporting Information S1). To illustrate results, we focus on 3 fjords from different regions of Greenland with a wide range of grounding-line depths and showing a generally good fit to observations for a single summer (2020; Figures 2a–2f). Comparing the full ensemble of modeled temperatures for Kangerlussuaq NW (purple shading in Figure 2a) with the observed profile (red profile), most model runs overestimate the warming of PW layers, but the best simulation within the ensemble (yellow profile) shows a much better match. The same behavior is seen for Itilliarsuup Kangerlua (Figure 2c), whereas Kangerlussuaq CE is more stratified, with the best simulation producing a deeper thermocline than the model mean (purple profile) and the observed profile (Figure 2e). Differences in salinity are relatively similar for the three fjords, with the model ensemble being overall fresher, and the best ensemble member following the observed profile more closely (Figures 2b, 2d, and 2f). Despite discrepancies between modeled and observed profiles, the model reproduces the observed differences between shelf and fjord temperature and salinity structures across all depths for most of the 90 simulated fjord-year combinations, save a few exceptions (Figures 2g and 2h; Figures S8–S19 in Supporting Information S1), with most best-fitting runs having RMSE for temperature and salinity below 0.5°C and 0.5 g/kg , respectively (Figure 2i).

Fjord temperature profiles typically differ from the shelf in characteristic ways, with a cooling of near-surface waters, a warming of the cooler PW layer, and limited impact on water properties below (Figure 2, Figures S8–S18 in Supporting Information S1). For example, the best FjordRPM simulation for Kangerlussuaq NW (Figure 2a) captures, in line with observations, the surface cooling of $\sim 3^\circ\text{C}$ and PW warming of $\sim 1^\circ\text{C}$, yielding a RMSE of $\sim 0.2^\circ\text{C}$ compared with observations. By varying the model parameters and comparing them with cases where the corresponding process is absent, we can identify the processes responsible for these characteristic impacts, and how the magnitude and nature of these impacts vary at different depths from fjord-to-fjord and year-to-year, as discussed in the following sections.

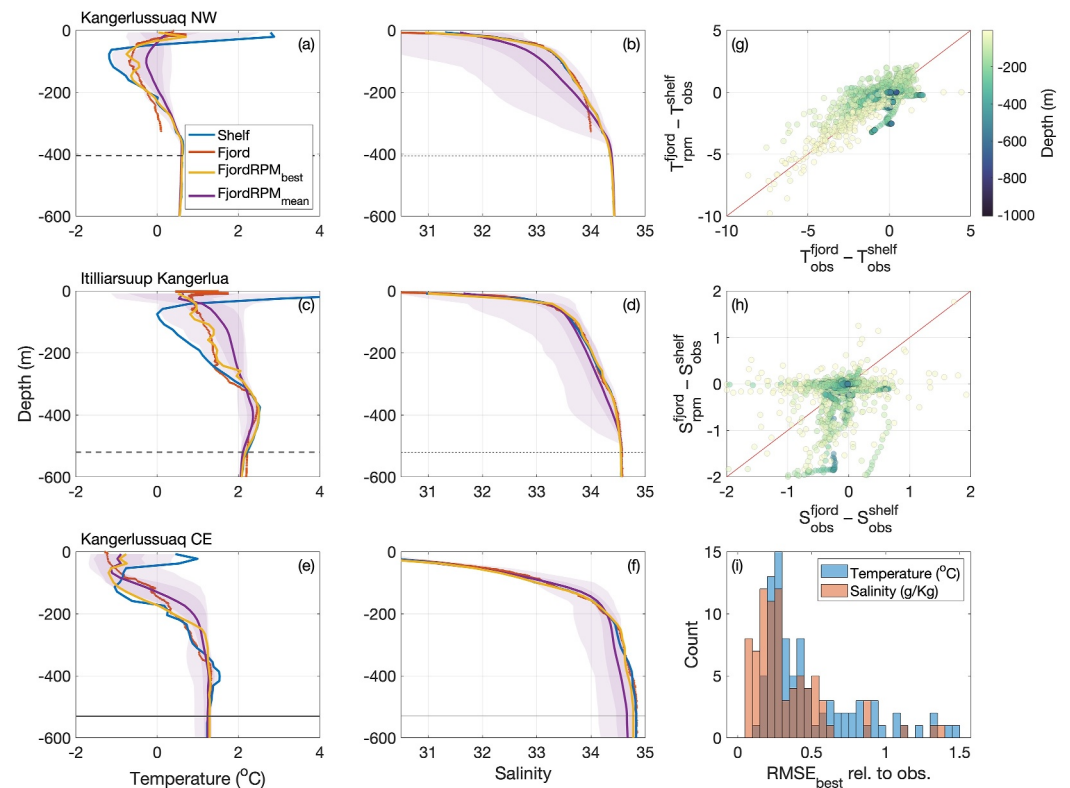


Figure 2. (a–f) Temperature and salinity profiles in early September (10-day average for the modeled profiles) for three example fjords (upper 600 m; rows). Blue lines show the shelf CTD, red lines show the fjord CTD, yellow lines show the best run for each fjord ensemble (considered to be the ensemble member with the smallest averaged normalized RMSE), and purple lines show the ensemble mean (lighter shading for the full ensemble spread, darker shading for the 1σ interval). Horizontal lines denote the sill (solid), and grounding-line (dashed) depths. Fjord names are listed in the top left corner of each row. Right column shows the correlation between observed and modeled differences between fjord and shelf (g) temperature and (f) salinity for the best performing ensemble member across all fjord depths, and panel (i) shows the frequency distribution of the temperature and salinity RMSEs for the best-performing fjord-year combinations.

3.2. Impacts of Fjord Processes

As expected, our sensitivity tests show all fjords cool at the surface under increased iceberg area (Figures 3a, 3d, and 3g). In all three example fjords, surface temperatures closely match those of the shelf in the absence of icebergs. Differences in surface temperature can be as high as 1.5°C between low and high iceberg conditions and over 2°C when icebergs are absent, with this impact decreasing with depth (Figures 3a, 3d, and 3g). The progressive cooling under increasing iceberg area is sub-linear, either because of the competing effect of iceberg meltwater-driven upwelling, which has a warming effect where fjord temperature increases with depth, or because the cooling caused by iceberg melt will itself limit further iceberg melting.

The ability of discharge plumes to warm or cool the fjord depends on where the plume reaches neutral buoyancy, and so which water masses will be mixed (Figures 3b, 3e, and 3h). This is in turn influenced by the grounding line depth (a physical characteristic of the fjord), the subglacial discharge (which can be estimated from data and models), and plume width (the least constrained property of the three), with narrower plumes entraining less ambient water and therefore able to reach shallower depths before finding neutral buoyancy (vertical lines in Figure 3). The variable impacts of plume upwelling can be seen in the example fjords, especially comparing how different plume widths compare with the no-subglacial discharge cases across different depths. At Kangerlussuaq NW, the plume reaches the surface during peak subglacial discharge (note the vertical bars in Figure 3 are an average over the entire melt season), and so impacts are concentrated in the upper water column where upwelling warms the PW layer and helps to counter the iceberg driven cooling of the surface layer (Figure 3b). Increasing the plume width serves only to amplify these effects, causing a net warming of the fjord. At Itilliarsuup Kangerlua, wider plumes find neutral buoyancy deeper below the surface, also increasing the warming of the PW layer but

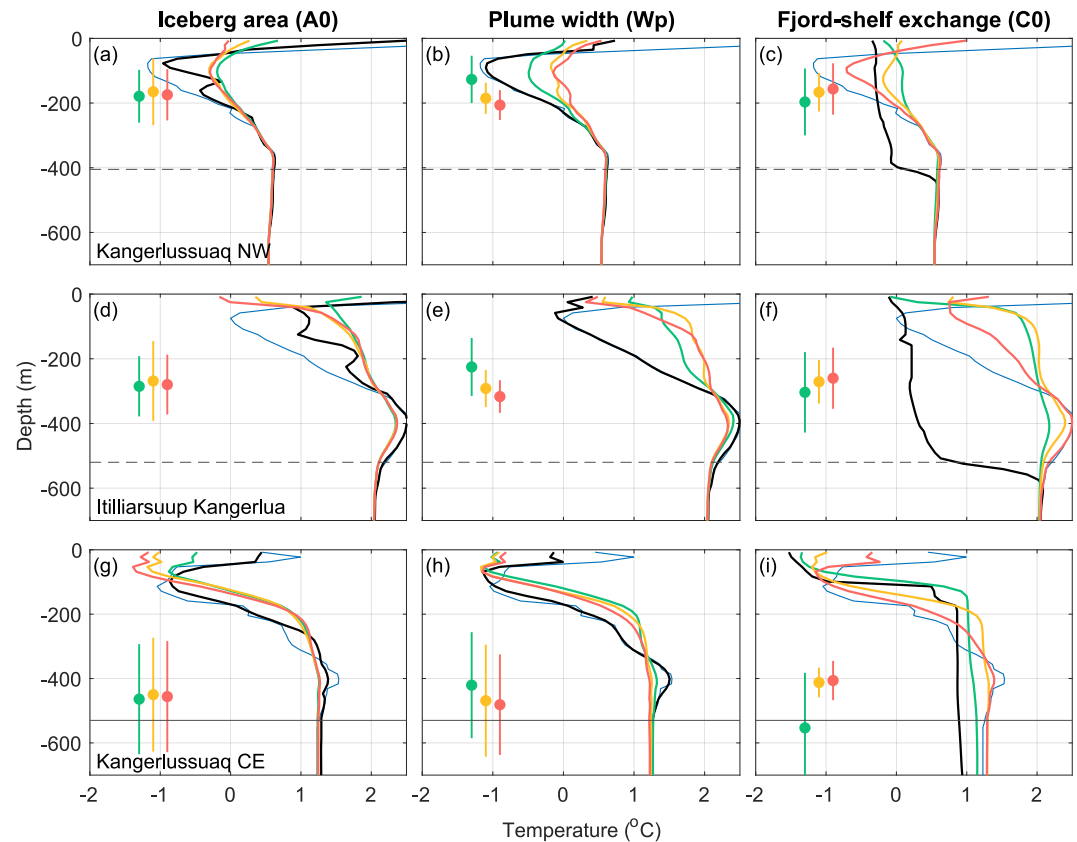


Figure 3. Temperature profiles for the three fjords (rows) in Figure 2, illustrating the impact of iceberg area (A_0), meltwater plume width (W_p), and fjord-shelf exchange (C_0). The blue lines are the shelf CTDs; green, yellow, and red lines show the mean modeled profile under low (below the 33rd percentile), medium (between the 33rd and 66th percentiles), and high (above the 66th percentile) values of the respective forcing. Black lines show a simulation where the respective forcing is either off or severely restricted, with average values for the other parameters (see main text). Vertical lines following the same coloring show the corresponding depth where the modeled meltwater-plume reaches neutral buoyancy over the melt season (2σ interval around the mean, marked by a circle). Horizontal dashed and solid lines as in Figure 2.

delivering less relatively warmer waters to the surface layer in comparison with Kangerlussuaq NW, with little net impact on fjord temperature (Figure 3e). At Kangerlussuaq CE, wider plumes do not rise fully into the PW layer, meaning their warming impact is limited (Figure 3h). It should be noted though that while the exact impacts of the plume vary, in all cases its effect is to decrease the temperature stratification, typically with a net warming impact on the fjord.

Increasing the fjord-shelf exchange coefficient acts as an opposing mechanism to iceberg melt and plume mixing. Higher exchange coefficients increase fluxes between fjord and shelf, replacing glacially-modified waters and bringing the fjord conditions closer to the shelf conditions, resulting in warmer surface waters and a cooler PW layer (Figures 3c, 3f, and 3i). The role of fjord-shelf exchanges on temperature stratification is most explicit in the end-member experiments where the exchange rate is reduced by ~ 3 orders of magnitude (effectively turning the fjord into a lake isolated from the ocean), resulting in a much more homogenous temperature profile above the grounding line for all example fjords. The balance of these impacts will, therefore, determine whether the result will be a net warming or cooling of the fjord.

Because direct communication between the fjord and shelf cannot take place below sill depth, water properties in this zone show limited time variation and are typically colder and fresher relative to water at equivalent depth on the shelf (Figures S9–S18 in Supporting Information S1). Similarly, minimal modification of fjord water properties is seen below grounding line depth: with no impact of ice melt or subglacial discharge below this depth, and time-constant shelf boundary conditions, there is only weak vertical mixing to drive change in this zone.

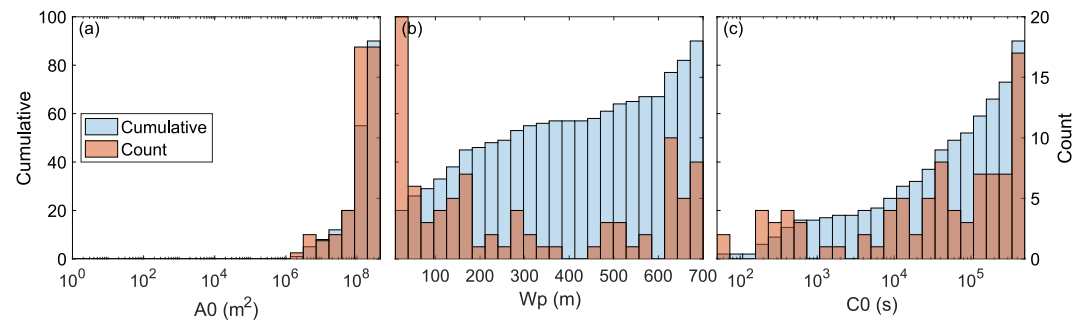


Figure 4. Distributions of best model parameters (a, iceberg area; b, meltwater plume width; c, fjord-shelf exchange coefficient) across all fjords and all years (brown). Blue bars denote the respective cumulative distributions. Horizontal axes span the entire parameter space evaluated for that parameter in this study.

3.3. Constraining Model Parameters From Observations

Considering only the best-fit ensemble member (i.e., smallest averaged normalized RMSE) for the fjord-year combination, some patterns emerge in the probability distributions of the parameter values despite considerable year-to-year (and fjord-to-fjord) variability (Figure 4). Best-fit parameter values typically increase toward the upper limit of the modeled range for iceberg concentration, illustrating both the importance of icebergs in driving surface cooling and the possibility that the current parameterization may underestimate melt rates (which could be separately addressed by adjusting the constant of proportionality between thermal forcing and melt; Slater et al. (2025)). Similarly, the distribution of shelf-exchange coefficients is skewed toward higher values, demonstrating the role of fjord-water renewal in preventing the glacial processes from completely homogenizing the water column. Conversely, meltwater-plume width has a more uniform distribution despite peaks at lower values. Nevertheless, ca. 50% of the best-fit fjords have plume widths <200 m, consistent with observations (Jackson et al., 2017). The relatively high number of fjords with much wider plumes may indicate instances where subglacial discharge is in reality split between multiple outlets, with similar effect to a single wider plume.

3.4. Toward a Greenland-Wide Fjord Assessment

A key advantage of FjordRPM is its computational efficiency: all 27,000 simulations can be run in less than 2 days using six cores on a mid-range laptop. Such efficiency means FjordRPM can be used to simulate relevant fjord processes at Greenland-wide scales over long timeframes at negligible computational cost compared with other physically based numerical models. While observations suitable for calibrating the model are not available for all fjords, the probability distributions in Figure 4 can be used to help select values which are likely to be appropriate in most cases, improving the assessment of poorly constrained fjords. For example, the difference in temperature RMSE between the best and worst performing simulations for the fjords in Figures 2 and 3 can vary from 0.3°C (Kangerlussuaq CE) to 0.78°C (Itilliarsuup Kangerlua). We expect that, as data availability increases, the model-parameter space can be better constrained, decreasing the uncertainty in the value ranges.

Despite promising model performance, the degree of success remains reliant on the availability of suitable forcing data. It is notable that we achieve a better fit to observations in western compared to eastern fjords (Figure 1b, Figures S8–S18 in Supporting Information S1). Given that the underpinning physical processes should be independent of location, this is most likely due to limitations of the data used to force the model. Water properties on the shelf in southeast Greenland are more spatially and temporally variable relative to the northwest, due to the confluence of major currents, strong gradients across the shelf, and more frequent storms (Harden et al., 2011; Jackson et al., 2014; Straneo et al., 2010). This means that the snapshot CTD data used to provide shelf boundary conditions for the model is less likely to be representative of water entering the fjord on seasonal timescales, highlighting a limitation in our ability to model these systems with current data. Despite recent efforts, data coverage inside and around Greenland fjords is still scarce, and even more limited in terms of their temporal cover. Year-round (Zahn et al., 2024) and winter (Hansen et al., 2025) measurements do exist, but are limited to a small subset of fjords. Similarly, the ability of the model to successfully simulate fjord water properties is dependent on accurate subglacial runoff inputs, which are in themselves model outputs with associated uncertainty, and exaggerated freshwater inputs may account for the simulation of overly fresh fjord conditions in some

instances (Figure 2h, Figures S16–S18 in Supporting Information S1). Similarly, the uncertainty around subglacial discharge, which affects plume neutral-buoyancy depth, could have affected our estimates of best plume-width values. Furthermore, a substantial mismatch between deep water properties in two fjords in NE Greenland (111 and 121, Figure S14 in Supporting Information S1) suggests inaccurate information on sill depths in these fjords. Despite our model being able to efficiently simulate fjords and capture water mass transformation due to glacial processes, more data around Greenland is needed to force the model, particularly for longer time periods and in a greater diversity of settings.

4. Summary and Conclusions

We used a reduced-physics model (FjordRPM) to simulate ensembles of 37 different fjords (totaling 27,000 model runs) for years with data availability between 2016 and 2020. Considering that fjords modulate the heat influx delivered to glacier fronts, we assessed how fjord temperatures respond to varying fjord iceberg area, meltwater-plume width, and fjord-shelf exchange rates. Using a subset of fjords, we demonstrated how increased iceberg area cools the fjord, whereas plume upwelling acts to decrease temperature stratification, while exchange with the shelf works to restore it. The depth at which the plume reaches neutral buoyancy (controlled by the grounding-line depth, subglacial discharge, plume width and fjord stratification) affects which water masses are mixed, resulting in a warmer fjord if AW is discharged in the PW layer. Conversely, enhanced exchanges with the shelf increase stratification, favoring the impact of shelf conditions (e.g., a larger PW layer, or warmer surface temperatures) on the fjord water-mass structure. Finally, constraining the model-parameter space using available observations further highlighted that our reduced-physics model can simulate fjords across all Greenland, but subject to the availability of adequate forcing data sets. We therefore stress the need for more oceanographic observations around Greenland, especially closer to fjord mouths, in order to better assess the role fjords play in modulating exchanges between the ice sheet and the ocean.

Data Availability Statement

Observations from CTD and AXCTD are available in OMG (2019, 2020), respectively. The subglacial discharge data set is available in Karlsson et al. (2022). A spreadsheet connecting all data sets to their respective fjords is available in Mas e Braga (2025a), and shapefiles containing the digitised fjord outlines and centrelines are available in Mas e Braga (2025a). FjordRPMv1.0 is archived in Slater et al. (2024), and a live version is kept in its GitHub repository <https://github.com/fjord-mix/fjordrpm>. All Matlab scripts used to compile the data, run the model, analyse the results, and plot the figures are available in Mas e Braga (2025b). Supplementary data sets are archived in Mas e Braga (2025a).

Acknowledgments

All authors acknowledge support from the UK Natural Environment Research Council (NERC) Grant NE/W00531X/1. DAS further acknowledges support from NERC Independent Research Fellowship NE/T011920/1.

References

- Böning, C. W., Behrens, E., Biastoch, A., Getzlaff, K., & Bamber, J. L. (2016). Emerging impact of Greenland meltwater on deepwater formation in the North Atlantic Ocean. *Nature Geoscience*, 9(7), 523–527. <https://doi.org/10.1038/ngeo2740>
- Cenedese, C., & Straneo, F. (2023). Icebergs melting. *Annual Review of Fluid Mechanics*, 55(1), 377–402. <https://doi.org/10.1146/annurev-fluid-032522-100734>
- Chu, V. W. (2014). Greenland ice sheet hydrology: A review. *Progress in Physical Geography: Earth and Environment*, 38(1), 19–54. <https://doi.org/10.1177/0309133313507075>
- Cowton, T. R., Slater, D. A., & Inall, M. E. (2023). Subglacial-discharge plumes drive widespread subsurface warming in Northwest Greenland's fjords. *Geophysical Research Letters*, 50(15), e2023GL103801. <https://doi.org/10.1029/2023GL103801>
- Cowton, T. R., Sole, A., Nienow, P., Slater, D. A., Wilton, D., & Hanna, E. (2016). Controls on the transport of oceanic heat to Kangerdlugssuaq Glacier, East Greenland. *Journal of Glaciology*, 62(236), 1167–1180. <https://doi.org/10.1017/jog.2016.117>
- Davison, B. J., Cowton, T., Sole, A., Cottier, F., & Nienow, P. (2022). Modelling the effect of submarine iceberg melting on glacier-adjacent water properties. *The Cryosphere*, 16(4), 1181–1196. <https://doi.org/10.5194/tc-16-1181-2022>
- De Andrés, E., Slater, D. A., Straneo, F., Otero, J., Das, S., & Navarro, I. (2020). Surface emergence of glacial plumes determined by fjord stratification. *The Cryosphere*, 14(6), 1951–1969. <https://doi.org/10.5194/tc-14-1951-2020>
- Enderlin, E. M., Hamilton, G. S., Straneo, F., & Sutherland, D. A. (2016). Iceberg meltwater fluxes dominate the freshwater budget in Greenland's iceberg-congested glacial fjords. *Geophysical Research Letters*, 43(21), 11287–11294. <https://doi.org/10.1002/2016GL070718>
- Fenty, I., Willis, J. K., Khazendar, A., Dinardo, S., Forsberg, R., Fukumori, I., et al. (2016). Oceans melting Greenland: Early results from NASA's ocean-ice mission in Greenland. *Oceanography*, 29(4), 72–83. <https://doi.org/10.5670/oceanog.2016.100>
- Fraser, N. J., & Inall, M. E. (2018). Influence of barrier wind forcing on heat delivery toward the Greenland ice sheet. *Journal of Geophysical Research: Oceans*, 123(4), 2513–2538. <https://doi.org/10.1002/2017JC013464>
- Gerrish, L. (2020). *The coastline of Kalaallit Nunaat/Greenland available as a shapefile and geopackage, covering the main land and islands, with glacier fronts updated as of 2017*. UK Polar Data Centre, Natural Environment Research Council, UK Research & Innovation. <https://doi.org/10.5285/8CECDE06-8474-4B58-A9CB-B820FA4C9429>

- Hager, A. O., Sutherland, D. A., & Slater, D. A. (2024). Local forcing mechanisms challenge parameterizations of ocean thermal forcing for Greenland tidewater glaciers. *The Cryosphere*, 18(2), 911–932. <https://doi.org/10.5194/tc-18-911-2024>
- Hansen, K., Karlsson, N. B., How, P., Poulsen, E., Mortensen, J., & Rysgaard, S. (2025). Winter subglacial meltwater detected in a Greenland fjord. *Nature Geoscience*, 18(3), 219–225. <https://doi.org/10.1038/s41561-025-01652-0>
- Harden, B. E., Renfrew, I. A., & Petersen, G. N. (2011). A climatology of wintertime barrier winds off Southeast Greenland. *Journal of Climate*, 24(17), 4701–4717. <https://doi.org/10.1175/2011JCLI4113.1>
- Inall, M. E., Murray, T., Cottier, F. R., Scharrer, K., Boyd, T. J., Heywood, K. J., & Bevan, S. L. (2014). Oceanic heat delivery via Kangerdlugssuaq Fjord to the south-east Greenland ice sheet. *Journal of Geophysical Research: Oceans*, 119(2), 631–645. <https://doi.org/10.1002/2013JC009295>
- Jackson, R. H., Motyka, R. J., Amundson, J. M., Abib, N., Sutherland, D. A., Nash, J. D., & Kienholz, C. (2022). The relationship between submarine melt and subglacial discharge from observations at a tidewater Glacier. *Journal of Geophysical Research: Oceans*, 127(10), e2021JC018204. <https://doi.org/10.1029/2021JC018204>
- Jackson, R. H., Shroyer, E. L., Nash, J. D., Sutherland, D. A., Carroll, D., Fried, M. J., et al. (2017). Near-glacier surveying of a subglacial discharge plume: Implications for plume parameterizations. *Geophysical Research Letters*, 44(13), 6886–6894. <https://doi.org/10.1002/2017GL073602>
- Jackson, R. H., Straneo, F., & Sutherland, D. A. (2014). Externally forced fluctuations in ocean temperature at Greenland glaciers in non-summer months. *Nature Geoscience*, 7(7), 503–508. <https://doi.org/10.1038/ngeo2186>
- Jakobsson, M., Mayer, L. A., Nilsson, J., Stranne, C., Calder, B., O'Regan, M., et al. (2020). Ryder Glacier in northwest Greenland is shielded from warm Atlantic water by a bathymetric sill. *Communications Earth & Environment*, 1(1), 1–10. <https://doi.org/10.1038/s43247-020-00043-0>
- Karlsson, N. B., Mankoff, K. D., & Solgaard, A. M. (2022). Greenland freshwater flux on glacier-basin scales [Dataset]. *GEUS Dataverse*. <https://doi.org/10.22008/FK2/BOVBVR>
- Karlsson, N. B., Mankoff, K. D., Solgaard, A. M., Larsen, S. H., How, P. R., Fausto, R. S., & Sørensen, L. S. (2023). A data set of monthly freshwater fluxes from the Greenland ice sheet's marine-terminating glaciers on a glacier-basin scale 2010–2020. *GEUS Bulletin*, 53(8338). <https://doi.org/10.34194/geusb.v53.8338>
- Mankoff, K. D., Straneo, F., Cenedese, C., Das, S. B., Richards, C. G., & Singh, H. (2016). Structure and dynamics of a subglacial discharge plume in a Greenlandic fjord. *Journal of Geophysical Research: Oceans*, 121(12), 8670–8688. <https://doi.org/10.1002/2016JC011764>
- Mas e Braga, M. (2025a). Supplementary datasets for Mas e Braga et al., “Controls on fjord temperature throughout Greenland in a reduced-physics model” [Dataset]. *Zenodo*. <https://doi.org/10.5281/ZENODO.15880691>
- Mas e Braga, M. (2025b). Fjord-mix/greenland-wide-drivers: V1.1 [Software]. *Zenodo*. <https://doi.org/10.5281/ZENODO.15880810>
- Millan, R., Rignot, E., Mouginot, J., Wood, M., Bjørk, A. A., & Morlighem, M. (2018). Vulnerability of Southeast Greenland glaciers to warm Atlantic water from Operation IceBridge and Ocean Melting Greenland data. *Geophysical Research Letters*, 45(6), 2688–2696. <https://doi.org/10.1002/2017GL076561>
- Moon, T., Fisher, M., Stafford, T., & Harden, L. (2023). QGreenland. *Zenodo*. <https://doi.org/10.5281/ZENODO.12823307>
- Morlighem, M. (2022). *IceBridge BedMachine Greenland, Version 5*. NASA National Snow and Ice Data Center Distributed Active Archive Center. <https://doi.org/10.5067/GMEVBWFLWA7X>
- Morlighem, M., Williams, C. N., Rignot, E., An, L., Arndt, J. E., Bamber, J. L., et al. (2017). BedMachine v3: Complete bed topography and ocean bathymetry mapping of Greenland from multibeam echo sounding combined with mass conservation. *Geophysical Research Letters*, 44(21), 11051–11061. <https://doi.org/10.1002/2017GL074954>
- Mortensen, J., Rysgaard, S., Bendtsen, J., Lennert, K., Kanzow, T., Lund, H., & Meire, L. (2020). Subglacial discharge and its down-fjord transformation in West Greenland fjords with an ice mélange. *Journal of Geophysical Research: Oceans*, 125(9), e2020JC016301. <https://doi.org/10.1029/2020JC016301>
- Mouginot, J., Rignot, E., Bjørk, A. A., van den Broeke, M., Millan, R., Morlighem, M., et al. (2019). Forty-six years of Greenland Ice Sheet mass balance from 1972 to 2018. *Proceedings of the National Academy of Sciences of the United States of America*, 116(19), 9239–9244. <https://doi.org/10.1073/pnas.1904242116>
- Nowicki, S., Goelzer, H., Seroussi, H., Payne, A. J., Lipscomb, W. H., Abe-Ouchi, A., et al. (2020). Experimental protocol for sea level projections from ISMIP6 stand-alone ice sheet models. *The Cryosphere*, 14(7), 2331–2368. <https://doi.org/10.5194/tc-14-2331-2020>
- OMG. (2019). OMG AXCTD profiles [Dataset]. *NASA Physical Oceanography Distributed Active Archive Center*. <https://doi.org/10.5067/OMGEV-AXCT1>
- OMG. (2020). OMG CTD conductivity temperature depth [Dataset]. *NASA Physical Oceanography Distributed Active Archive Center*. <https://doi.org/10.5067/OMGEV-CTDS1>
- Sanchez, R., Straneo, F., Hughes, K., Barbour, P., & Shroyer, E. (2024). Relative roles of plume and coastal forcing on exchange flow variability of a glacial fjord. *Journal of Geophysical Research: Oceans*, 129(6), e2023JC020492. <https://doi.org/10.1029/2023JC020492>
- Slater, D. A., Felikson, D., Straneo, F., Goelzer, H., Little, C. M., Morlighem, M., et al. (2020). Twenty-first century ocean forcing of the Greenland ice sheet for modelling of sea level contribution. *The Cryosphere*, 14(3), 985–1008. <https://doi.org/10.5194/tc-14-985-2020>
- Slater, D. A., Johnstone, E., Mas e Braga, M., Fraser, N., Cowton, T., & Inall, M. (2024). Fjord-mix/fjordrpm: FjordRPM release for GMD submission [Software]. *Zenodo*. <https://doi.org/10.5281/ZENODO.14536606>
- Slater, D. A., Johnstone, E., Mas e Braga, M., Fraser, N., Cowton, T., & Inall, M. (2025). FjordRPM v1.0: A reduced-physics model for efficient simulation of glacial fjords. *EGU sphere*, 1–38. <https://doi.org/10.5194/egusphere-2024-3934>
- Slater, D. A., Straneo, F., Felikson, D., Little, C. M., Goelzer, H., Fettweis, X., & Holte, J. (2019). Estimating Greenland tidewater glacier retreat driven by submarine melting. *The Cryosphere*, 13(9), 2489–2509. <https://doi.org/10.5194/tc-13-2489-2019>
- Song, C., & Kawai, R. (2023). Monte Carlo and variance reduction methods for structural reliability analysis: A comprehensive review. *Probabilistic Engineering Mechanics*, 73, 103479. <https://doi.org/10.1016/j.probengmech.2023.103479>
- Straneo, F., & Cenedese, C. (2015). The dynamics of Greenland's glacial fjords and their role in climate. *Annual Review of Marine Science*, 7(1), 89–112. <https://doi.org/10.1146/annurev-marine-010213-135133>
- Straneo, F., Hamilton, G. S., Sutherland, D. A., Stearns, L. A., Davidson, F., Hammill, M. O., et al. (2010). Rapid circulation of warm subtropical waters in a major glacial fjord in East Greenland. *Nature Geoscience*, 3(3), 182–186. <https://doi.org/10.1038/ngeo764>
- Straneo, F., Sutherland, D. A., Holland, D., Gladish, C., Hamilton, G. S., Johnson, H. L., et al. (2012). Characteristics of ocean waters reaching Greenland's glaciers. *Annals of Glaciology*, 53(60), 202–210. <https://doi.org/10.3189/2012AoG60A059>
- Sutherland, D. A., & Straneo, F. (2012). Estimating ocean heat transports and submarine melt rates in Sermilik Fjord, Greenland, using lowered acoustic Doppler current profiler (LADCP) velocity profiles. *Annals of Glaciology*, 53(60), 50–58. <https://doi.org/10.3189/2012AoG60A050>

- Uotila, P., Goosse, H., Haines, K., Chevallier, M., Barthélemy, A., Bricaud, C., et al. (2019). An assessment of ten ocean reanalyses in the polar regions. *Climate Dynamics*, 52(3), 1613–1650. <https://doi.org/10.1007/s00382-018-4242-z>
- Wood, M., Khazendar, A., Fenty, I., Mankoff, K., Nguyen, A. T., Schulz, K., et al. (2024). Decadal evolution of ice-ocean interactions at a Large East Greenland glacier resolved at fjord scale with downscaled ocean models and observations. *Geophysical Research Letters*, 51(7), e2023GL107983. <https://doi.org/10.1029/2023GL107983>
- Zahn, M. J., Laidre, K. L., Simon, M., Stafford, K. M., Wood, M., Willis, J. K., et al. (2024). Consistent seasonal hydrography from moorings at Northwest Greenland glacier fronts. *Journal of Geophysical Research: Oceans*, 129(9), e2024JC021046. <https://doi.org/10.1029/2024JC021046>